



## Analysis of the Stream Function for Peristaltic Flow of Jeffrey Fluid Under the Influence of Rotation and Electric Field in Porous Medium

Malath Sagban Abied \*, Liqaa Zeki Hummady

Department of Mathematics, College of Science, University of Baghdad, Baghdad, Iraq

Received: 28/6/2024

Accepted: 22/1/2025

Published: 30/1/2026

### Abstract

This article examines how the rotation variable and other variables affect the Jeffrey fluid's peristaltic flow through a porous medium in an asymmetric channel under the influence of an electric field, foundational equations following the Jeffrey fluid model were used. The flow analysis is based on the long-wavelength assumption and low Reynolds number assumptions, and the governing partial differential equations of the system were solved using the approximate analytical perturbation method. Mathematical expressions are used to represent the pressure gradient, axial velocity distributions, and stream function, with the most influential parameters identified as velocity, pressure, and stream function. Examples of these parameters include the Helmholtz-Smoluchowski number, Darcy number, and rotation element. It was observed that some parameters lead to an increase in velocity, while others cause a decrease, and the same applies to pressure. Graphs are used to represent velocity, pressure gradient, and their effect on the parameters influencing the equations of motion. Using a set of numbers to produce numerical results, the impact of different parameters is explored, as illustrated in the graphs. The MATHEMATICA software was used to achieve these results.

**Keywords:** Peristaltic flow, Rotation, Velocity, Stress, Electric field.

## تأثير الدوران على التدفق التمعجي لسائل جيفرى بوجود المجال الكهربائي قناة غير متماثلة مع وسط مسامي

ملاذ سكبان عبد \* ، لقاء زكي حمادي

قسم الرياضيات ، كلية العلوم ، جامعة بغداد ، بغداد ، العراق

### الخلاصة

يبحث هذا المقال في كيفية تأثير متغير الدوران والمتغيرات الأخرى على تدفق سائل جيفرى الحركي عبر وسط مسامي في قناة غير متماثلة تحت تأثير مجال كهربائي، تم استخدام معادلات تأسيسية تتبع نموذج سائل جيفرى. يعتمد تحليل التدفق على فرضية الطول الموجي الطويل وافتراضات العدد رينولدز المنخفض، وتم حل المعادلات التفاضلية الجزئية الحاكمة للنظام باستخدام طريقة الاضطراب التفريضية التحليلية. تستخدم التعبيرات الرياضية تمثيلاً عن تدرج الضغط، وتوزيعات السرعة المحورية، ودالة الانسياب، وتم تحديد المعلمات الأكثر تأثيراً مثل السرعة، والضغط، ودالة الانسياب. من أمثلة هذه المعلمات عدد هيلموليتر -

\*Email: [malathsagban@gmail.com](mailto:malathsagban@gmail.com)

مسؤول خويفي، وعدد دارسي، وعنصر الدوران، وقد لوحظ أن بعض المعلمات تؤدي إلى زيادة في السرعة وأخرى تؤدي إلى انخفاضها، وينطبق نفس الأمر على الضغط. تستخدم الرسوم البيانية للتغيير عن السرعة ودرج الضغط ودالة الجريان وتأثيرهما على المعلمات المؤثرة في معادلات الحركة. باستخدام مجموعة من الأعداد لإنتاج نتائج رقمية، يتم استكشاف تأثير مختلف المعلمات كما هو موضح بالرسم البياني. تم استخدام البرنامج الرياضي MATHEMATICA لتحقيق هذه النتائج.

## 1. Introduction

Via a process called peristaltic transport, fluid is transported by means of wave trains that go through the channel. Chyme moving through the digestive tract, ovum being transferred, urine being delivered through the ureter, lymph traveling through the lymphatic arteries, blood passing through the bile duct, and food being swallowed. This phenomenon has numerous applications in body structure and biomedical engineering, including other real-world usage. First of all, A. M. Abd-Alla and S. M. Abo-Dahab [1], and R. S. Kareem and A. M. Abduhadi [2] explored two different scenarios to investigate peristaltic transport: one focused on peristaltic flow in asymmetric channel and the other one study the peristaltic flow in inclined channel. Z. A. Jaafari, L. Hummady and M.H. Thaw [3], S. Akram and S. Nadeem [4], A. W. Salih [5], and D. Gamachu and W. Ibrahim [6] looked into the peristaltic transport process, which has drawn interest from many scholars. Furthermore, many industrial and physiological processes are more familiar with non-Newtonian fluids than with viscous liquids [7-10]. The Jeffrey liquid is the most fundamental linear model among these materials that deals with the non-Newtonian fluid properties for which analytical or precise solutions are theoretically possible. Geo-fluid dynamics, biomechanics, and engineering are three fields in which fluid flow through porous media is particularly relevant. In the human physiological systems, these fluxes are observed in the kidneys, lungs, small blood vessels, cartilage, bones, etc. One might imagine the human body's tissues as porous, pliable material [11], [12] and [13]. To function, they need to be able to transfer blood and other nutrients. Scientists have simulated the flow of Newtonian and non-Newtonian fluids across porous surfaces to detect a variety of disorders, including tumor growth. Several recent the phenomenon of rotation has multiple applications in geophysical and cosmic fluxes. In addition, rotation helps us understand the behavior of ocean circulation and the evolution of galaxies. Investigations of the orientation of nanoparticles in fluid systems are also conducted by rotating diffusion. In rotational spectroscopy, rotation is also utilized to quantify the energy of transitions between quantized rotational states of gas phase molecules. One flow scenario where the peristalsis of fluid in the presence of rotation is particularly significant is the movement of physiological fluids, such as blood and saline water [14], [15] and [16]. The movement of biofluid in the ureters, arterioles, and intestines is clearly aided by the rotation field. In order to analyze the impacts, the rotation in the electric field in an asymmetric porous media channel a mathematical model must be developed. There are five sections in this study. In order to facilitate the governing equations with the assumption of a very long wavelength or a very small Reynolds number in order to solve the problem, the governing equations with the boundary conditions are formed and the dimensionless transformations are displayed in the first part. The dimensionless equations are analytically solved using the perturbation method in the following section, providing the Jeffrey fluid's electric distribution, velocity profile, pressure gradient, and stream function equations. The third section describes the effects of altering the fourth section solved the equation. The final section provides a quick summary of the three main variables (Jeffrey parameter, Darcy number, and electric parameter) that affect the fluid's velocity [17], [18] and S. R. Mahmoud, [19] conducted research on the impact of rotation and peristaltic motion of Jeffrey fluid in a porous medium under the influence of a magnetic field. Our study focuses on the effect of an

electric field on the fluid due to its significance in various fields, such as its importance in neural signaling for cerebrospinal fluid. The objective of this research is to examine the peristalsis in transport of Jeffrey fluid when there is rotation, porous medium, electric field, The velocity of the fluid increases with an increase in the electrical coefficient, and this benefits us in real-life applications, for example in electrohydraulic therapy electric fields are used to direct the flow of medical fluids in the body to stimulate healing or improve the distribution of medications.

## 2. Problem mathematical description

The peristaltic motion is incompressible motion to Jeffrey fluid with width ( $d' + d$ ) in a two-dimensional asymmetric channel. The endless sinewave that flows and travels along the walls of the channel, what is the forward motion ( $c$ ) that produces the flow. The geometric definition of the wall structure is:

$$\bar{h}_1(\bar{x}, \bar{t}) = d - a_1 \sin[(\bar{x} - c\bar{t})] \quad \text{upper wall.} \quad (1)$$

$$\bar{h}_2(\bar{x}, \bar{t}) = -d' - a_2 \sin[(\bar{x} - c\bar{t}) + \theta] \quad \text{lower wall.} \quad (2)$$

We  $h_1(\bar{x}, \bar{t})$  and  $h_2(\bar{x}, \bar{t})$  are the lower and upper walls, respectively, where ( $d, d'$ ) represents the channel's width, ( $a_1, a_2$ ) waves are amplified, ( $\lambda$ ) is wave length, ( $c$ ) is the velocity of the wave, and ( $\phi$ ) the speed of the waves ( $0 \leq \phi \leq \pi$ ), then  $\phi = 0$ , is an out-of-phase channel that is symmetric, also  $\phi = \pi$  waves are in phase, and of square-shaped coordinates is selected to that ( $\bar{X}$ -axis) pointing in the wave's direction, and ( $\bar{Y}$ -axis) is perpendicular to  $\bar{X}$ , with  $\bar{t}$  representing the time.

$$a_1^2 + a_2^2 + 2a_1a_2 \cos \phi \leq (d' + d)^2$$

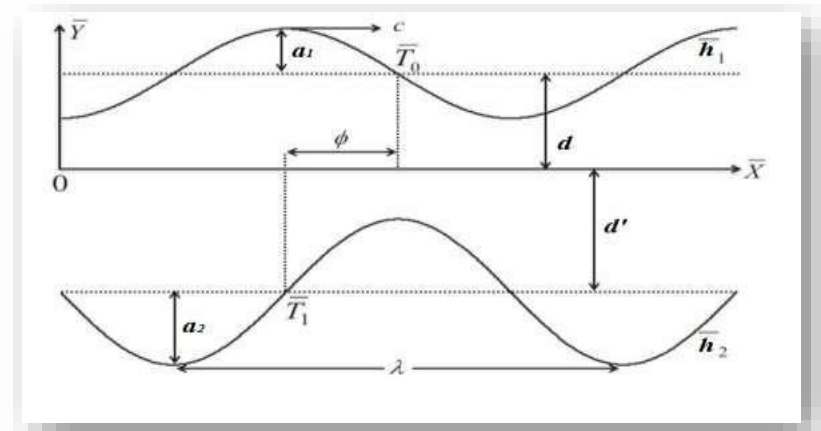


**Figure 1:** Coordinates of Asymmetric Cartesian Dimensional Channels.

It is also presumed that the walls do not move longitudinally. This assumption restricts the deformation capacity of the walls; it does not imply that the channel remains rigid during longitudinal motions.

## 3. Basic equation

The Cauchy stress tensor  $\bar{S}$  for a fluid that obeys the Jeffery model [20], is provided below

$$\bar{S}_{ij} = \frac{1}{(1+\lambda_1)} (Y^i + \lambda_2 \dot{Y}^i) \quad (3)$$

$$\dot{Y}^i = \nabla \bar{V}^i + \nabla \bar{V}^{i\perp} \quad (4)$$

$$\ddot{Y} = \frac{\partial \dot{Y}}{\partial X} + (\nabla \cdot \bar{V}) \dot{Y} \quad (5)$$

$$\nabla \cdot \bar{V} = \frac{\partial \bar{U}}{\partial \bar{X}} + \frac{\partial \bar{V}}{\partial \bar{Y}}. \quad (6)$$

Where  $\dot{Y}$  is the shear rate,  $\lambda_2$  is the retardation time,  $\lambda_1$  is the ratio relaxation time and  $(\dot{Y})$  represent differential of  $(Y)$ .  $(\nabla \bar{V})$  Given the Cartesian coordinate system  $(x, y)$  and  $(\nabla \bar{V})^T$ , is the fluid velocity in the Cartesian coordinates system  $(x, y)$

$$\bar{s}_{\bar{x}\bar{x}} = \frac{1}{1+\lambda_1} (2\bar{u}_{\bar{x}} + \lambda_2 (2\bar{u}_{\bar{x}\bar{x}} + 2\bar{u}_{\bar{x}}\bar{v}_{\bar{y}})) \quad (7)$$

$$\bar{s}_{\bar{x}\bar{y}} = \frac{1}{1+\lambda_1} ((\bar{u}_{\bar{y}} + \bar{v}_{\bar{x}}) + \lambda_2 ((\bar{u}_{\bar{x}} + \bar{v}_{\bar{y}})(\bar{u}_{\bar{y}} + \bar{v}_{\bar{x}}))) \quad (8)$$

$$\bar{s}_{\bar{y}\bar{x}} = \frac{1}{1+\lambda_1} ((\bar{u}_{\bar{y}} + \bar{v}_{\bar{x}}) + \lambda_2 ((\bar{u}_{\bar{x}} + \bar{v}_{\bar{y}})(\bar{u}_{\bar{y}} + \bar{v}_{\bar{x}}))). \quad (9)$$

#### 4. The governing equation

Three pair nonlinear partial differentials of continuity and momentum, expressed in an affixed frame  $(X, Y)$ , control the flow with the laboratory serving as a point of reference, [21] the following equations govern flow:

The equation for continuity.

$$\frac{\partial \bar{U}}{\partial \bar{X}} + \frac{\partial \bar{V}}{\partial \bar{Y}} = 0. \quad (10)$$

In X-axis

$$\rho \left( \frac{\partial}{\partial \bar{t}} + \bar{U} \frac{\partial}{\partial \bar{X}} + \bar{V} \frac{\partial}{\partial \bar{Y}} \right) \bar{U} - \rho \Omega \left( \Omega \bar{u} + 2 \frac{\partial \bar{V}}{\partial \bar{t}} \right) = - \frac{\partial \bar{p}}{\partial \bar{X}} + \frac{\partial}{\partial \bar{X}} \bar{s}_{\bar{x}\bar{x}} + \frac{\partial}{\partial \bar{Y}} \bar{s}_{\bar{x}\bar{y}} + \bar{p}_c E_x - \frac{\mu_0}{k} \bar{U} \quad (11)$$

In Y-axis

$$\rho \left( \frac{\partial}{\partial \bar{t}} + \bar{U} \frac{\partial}{\partial \bar{X}} + \bar{V} \frac{\partial}{\partial \bar{Y}} \right) \bar{V} - \rho \Omega \left( \Omega \bar{v} + 2 \frac{\partial \bar{U}}{\partial \bar{t}} \right) = - \frac{\partial \bar{p}}{\partial \bar{Y}} + \frac{\partial}{\partial \bar{X}} \bar{s}_{\bar{x}\bar{y}} + \frac{\partial}{\partial \bar{Y}} \bar{s}_{\bar{y}\bar{y}} + \bar{p}_c E_y - \frac{\mu_0}{k} \bar{V}. \quad (12)$$

The Famous Poisson Equation

$$\begin{aligned} p_c &= -\epsilon \nabla^2 \bar{\phi} \\ \bar{\phi} &= \text{electric potential} \\ \bar{\phi}(y) &= \frac{\sinh(y+h)k}{\sinh(2hk)}. \end{aligned} \quad (13)$$

Where the  $(\rho)$ ,  $(\bar{u})$ ,  $(\bar{v})$ ,  $(\bar{y})$ ,  $(\bar{p})$ ,  $(\mu)$ ,  $(k)$ ,  $(\epsilon E_x)$ ,  $(\Omega)$  are the fluid density, axial velocity, transverse velocity, transverse coordinate, pressure, dynamic viscosity, permeability parameter, constant electric field, and rotation.

In the laboratory frame  $(\bar{x}, \bar{y})$ , the flow is unstable; in the wave frame  $(\bar{X}, \bar{Y})$ , a coordinate system moving at wave speed  $(c)$  experiences steady motion. The subsequent phrases

$$\begin{aligned} \bar{X} &= \bar{x} - c\bar{t}, \bar{Y} = \bar{y}, \bar{U}(\bar{X}, \bar{Y}) = \bar{u}(\bar{x}, \bar{y}) - c, \bar{V}(\bar{X}, \bar{Y}) = \bar{v}(\bar{x}, \bar{y}), \bar{T}(\bar{X}, \bar{Y}) = \bar{T}(\bar{x}, \bar{y}, \bar{t}), \bar{P}(\bar{X}, \bar{Y}) \\ &= \bar{P}(\bar{x}, \bar{y}) \end{aligned} \quad (14)$$

wherever  $(\bar{U}, \bar{V})$  indicate the speed  $\bar{p}$  is a symbol for the pressure inside the wave frame. Now, we swap out Equation (14) into formulas (1) (2) and (7-12) and add the non-dimensional variables to the final equation to normalize it.

$$\begin{aligned} x &= \frac{1}{\lambda} \bar{x}, y = \frac{1}{d} \bar{y}, u = \frac{1}{c} \bar{u}, v = \frac{1}{\delta c} \bar{v}, t = \frac{c}{\lambda} \bar{t}, \delta = \frac{d}{\lambda}, Re = \frac{\rho c d}{\mu}, Da = \frac{k}{d^2}, s_{xx} = \frac{\lambda}{\mu c} \bar{s}_{\bar{x}\bar{x}} \\ s_{xy} &= \frac{d}{\mu c} \bar{s}_{\bar{x}\bar{y}}, s_{yy} = \frac{d}{\mu c} \bar{s}_{\bar{y}\bar{y}}, h_1 = \frac{1}{d} \bar{h}_1, Uhs = \frac{-E_x \epsilon \epsilon}{\mu_0 c}, h_2 = \frac{1}{d} \bar{h}_2, \end{aligned} \quad (15)$$

where the wave number is ( $\delta$ ), the Darcy number is (Da), the Helmholtz-Smoluchowski velocity is (Uhs), and the Reynold number is (Re). The following non-dimensional variables have been used to normalize the resultant equation after Equation (15) have been replaced into Equations (10), (11) and (12)

$$\begin{aligned} \text{Re}\delta \left( \frac{\partial u}{\partial t} + u \frac{\partial u}{\partial x} + v \frac{\partial u}{\partial y} \right) - \frac{\rho d^2 \Omega^2}{\mu} u - \frac{d^2 c}{\mu} \delta \frac{\partial v}{\partial t} \\ = - \frac{\partial p}{\partial x} + \delta d \frac{\partial s_{xx}}{\partial x} + d \frac{\partial s_{xy}}{\partial y} + \delta^2 \frac{\epsilon E_x \epsilon}{\mu c} \frac{\partial^2 \phi}{\partial x^2} - Uhs \frac{\partial^2 \phi}{\partial y^2} \\ - \frac{d^2}{k} u \end{aligned} \quad (16)$$

$$\begin{aligned} \frac{\partial p}{\partial x} = \frac{\rho \Omega^2 d^2}{\mu} u + \frac{\partial s_{xy}}{\partial y} - Uhs \frac{\partial^2 \phi}{\partial y^2} \\ - \frac{1}{Da} u \end{aligned} \quad (17)$$

$$\begin{aligned} \text{Re} \delta^3 \left( \frac{\partial v}{\partial t} + u \frac{\partial v}{\partial x} + v \frac{\partial v}{\partial y} \right) - \frac{\rho d^2}{\mu} \delta^2 \Omega^2 v - \frac{2 \Omega \delta^2 \text{Re}}{\lambda} \left( \frac{\partial u}{\partial t} \right) \\ = - \frac{\partial p}{\partial y} + \delta^2 \frac{\partial}{\partial x} \tau_{xy} + \delta \frac{\partial}{\partial y} \tau_{yy} + Uhs \left( \delta^2 \frac{\partial^2 \phi}{\partial x^2} + \frac{\partial^2 \phi}{\partial y^2} \right) \\ - v \delta^2 \left( \frac{1}{Da} \right) \end{aligned} \quad (18)$$

$$\frac{\partial p}{\partial y} = 0. \quad (19)$$

The Equation (8) becomes:

$$s_{xy} = \frac{1}{1+\lambda_1} \left[ \frac{c}{d} \frac{\partial u}{\partial y} + \lambda_2 \left( \left( \frac{c}{d} \frac{\partial u}{\partial x} \right) \left( \frac{c}{d} \frac{\partial u}{\partial y} \right) \right) \right]. \quad (20)$$

The Equation (12) becomes:

$$\frac{\partial p}{\partial x} = \frac{\rho \Omega^2 d^2}{\mu} u + \frac{c}{1+\lambda_1} \left( \frac{\partial^2 u}{\partial y^2} \right) - Uhs \frac{\partial^2 \phi}{\partial y^2} - \frac{1}{Da} u \quad (21)$$

$$\text{Let } \alpha = \frac{c}{1+\lambda_1} \quad \xi = \frac{\rho \Omega^2 d^2}{\mu}. \quad (22)$$

By derivation Equation (21) respect to (y)

$$\begin{aligned} \xi \frac{\partial u}{\partial y} + \alpha \frac{\partial^3 u}{\partial y^3} - Uhs \frac{\partial^3 \phi}{\partial y^3} - \frac{1}{Da} \frac{\partial u}{\partial y} \\ = 0. \end{aligned} \quad (23)$$

The stream function ( $\psi$ ) is connected with the velocity components by the relations

$$\text{Let } u = \frac{\partial \psi}{\partial y} \quad \text{and} \quad v = - \frac{\partial \psi}{\partial x}. \quad (24)$$

$$\left( \xi - \frac{1}{Da} \right) \frac{\partial^2 \psi}{\partial y^2} + \alpha \frac{\partial^4 \psi}{\partial y^4} - Uhs \frac{\partial^3 \phi}{\partial y^3} = 0. \quad (25)$$

Substitution Equation (24) in continuity Equation

$$\frac{\partial^2 \psi}{\partial x \partial y} - \frac{\partial^2 \psi}{\partial x \partial y} = 0. \quad (26)$$

The wave frame's dimensionless boundary conditions are:

$$\Psi = \frac{F}{2}, \frac{\partial \Psi}{\partial y} = -1 \text{ at } y = h_1, \quad \Psi = \frac{-F}{2}, \frac{\partial \Psi}{\partial y} = -1 \text{ at } y = h_2 \quad (27)$$

## 5. Resolution of the issue

With all of the arbitrary parameters, an accurate result is unattainable. To obtain the solution, we utilize the perturbation approach. We then discuss the solution to the disturbance.

$$\begin{aligned} \Psi &= \Psi_0 + \alpha \Psi_1 + O(\alpha^2) \\ P &= P_0 + \alpha P_1 + O(\alpha^2) \\ F &= F_0 + \alpha F_1 + O(\alpha^2). \end{aligned} \quad (28)$$

Substitute the terms Equation (28) into Equation (25) together with the boundary conditions Equation (27) ( $\delta \ll 1$ ). The following system of equations is produced by equating the coefficients of equivalent powers of ( $\alpha$ ), where the higher order terms involving the power of  $\delta$  are smaller and hence unimportant.

### 5.1 Order zero system

In the zeroth order system, we obtain: when the terms of order ( $\alpha$ ) are small

$$\begin{aligned} \xi \Psi_{0yy} - U_{hs} \emptyset_{yyy} - \frac{1}{Da} \Psi_{0yy} &= 0 \\ \Psi_0 = \frac{F_0}{2}, \frac{\partial \Psi_0}{\partial y} &= -1 \text{ at } y = h_1 \quad \text{and} \quad \Psi_0 = -\frac{F_0}{2}, \frac{\partial \Psi_0}{\partial y} = -1 \text{ at } y = h_2. \end{aligned} \quad (29)$$

### 5.2 Order first system

$$\begin{aligned} \xi \Psi_{1yy} + \Psi_{0yyyy} &= 0. \\ \Psi_1 = \frac{F_1}{2}, \frac{\partial \Psi_1}{\partial y} &= -1 \text{ at } y = h_1 \quad \text{and} \quad \Psi_1 = -\frac{F_1}{2}, \frac{\partial \Psi_1}{\partial y} = -1 \text{ at } y = h_2 \\ \Psi &= \Psi_0 + \alpha \Psi_1. \end{aligned} \quad (30)$$

## 6. The findings and discussion

The primary focus of this study is how fluid flow in a porous medium is affected by Darcy number (Da), (Uhs) Helmholtz-smoluchowsk, ( $\alpha$ ) parameter of Jeffrey fluid and other parameters in the presence of an electric field on the pressure( P) and velocity curves (U) and the stream function ( $\psi$ ). Even studied (M. Kothandapani 2008) the same effects in the presence of magnetic fields, our study it looks at the impact of an electric field, which allows us to learn more about the relevant physical processes. We intend to compare the results with those of previous studies and provide more insight into how different parameters impact flow behavior in these complex systems.

## 7. Pressure gradient dp/dx:

The Figures (2 – 8) are portrayed to analyze the various vital parameters on pressure gradient (Da,  $\Omega$ , uhs,  $c$ ,  $\rho$ ,  $\alpha$ ,  $\mu$ , ) where the dp/dx refer to the change in axial pressure gradient across the channel

- It is clear from Figures (2), (5), and (6) that as the Darcy number (Da), rotation rate ( $\Omega$ ), and Jeffrey fluid parameter ( $\alpha$ ) increase, so does the pressure gradient. The effect becomes more noticeable at increasing (Da) values. Greater permeability is indicated by a bigger Darcy number, which makes it easier for fluid to flow through porous material, lowering flow resistance and enhancing the pressure gradient. Centrifugal forces intensify this gradient as a result of rotation, particularly in situations where there is little flow resistance because of high permeability. The elastic properties of the fluid are reflected in the Jeffrey fluid parameter ( $\alpha$ ). The fluid's elasticity increases with Jeffrey fluid parameter, improving its sensitivity to rotating forces and raising the pressure gradient.

- Figure (3) illustrates how the pressure gradient decreases as the Helmholtz-Smoluchowski value ( $U_{hs}$ ) increases. This is because of the fluid's electrokinetic effects, which reduce the pressure needed to keep the fluid moving by enhancing electroosmotic flow with increasing  $U_{hs}$  values. The pressure gradient is countered by electrokinetic forces, which less strength.
- In Figures (4) and (7) steady pressure gradient is produced by increases in viscosity ( $\mu$ ) and density ( $\rho$ ), as seen Density has an impact on the fluid's inertia, but viscosity raises the internal resistance to flow. But when both variables increase in proportion, they counteract one another and keep the pressure gradient constant. Because viscosity and density affect resistive and driving forces in tandem, they can balance out variations to maintain a constant pressure gradient under a range of circumstances.

## 8. Stream function( $\psi$ )

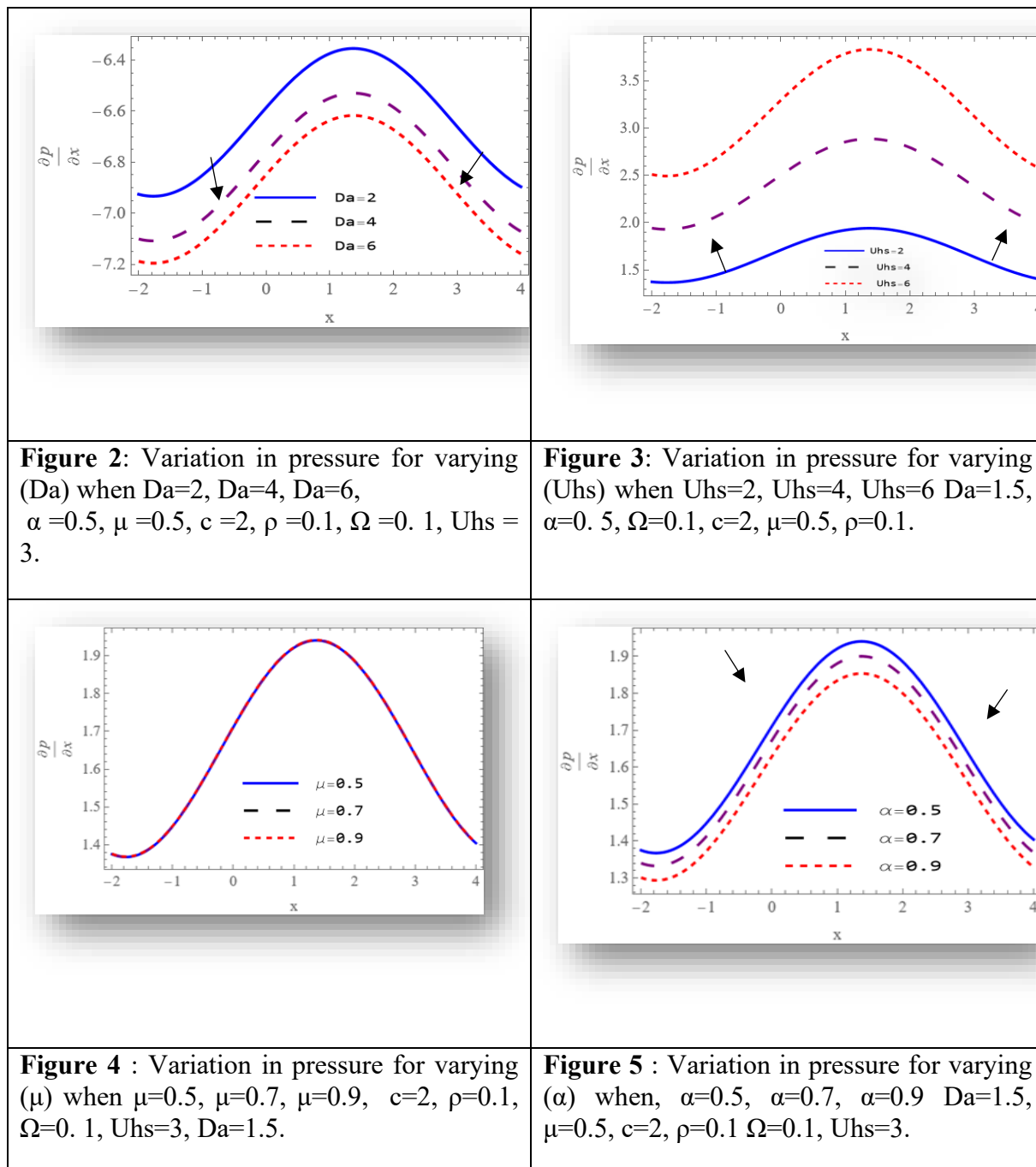
The changing values of stream function is reflects the variation to changing the values of ( $Da, \Omega, U_{hs}, c, \rho, \alpha, \mu$ ),

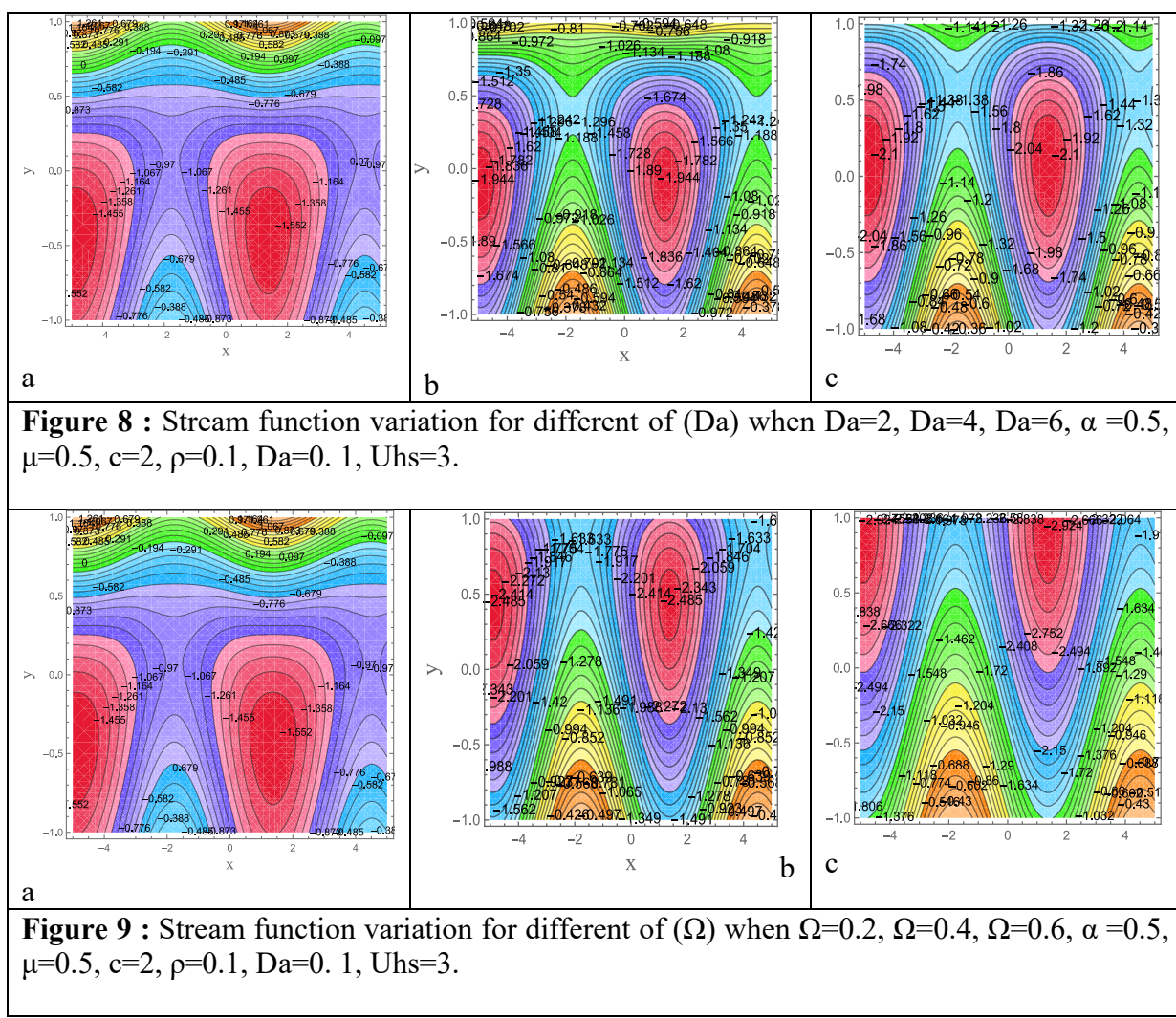
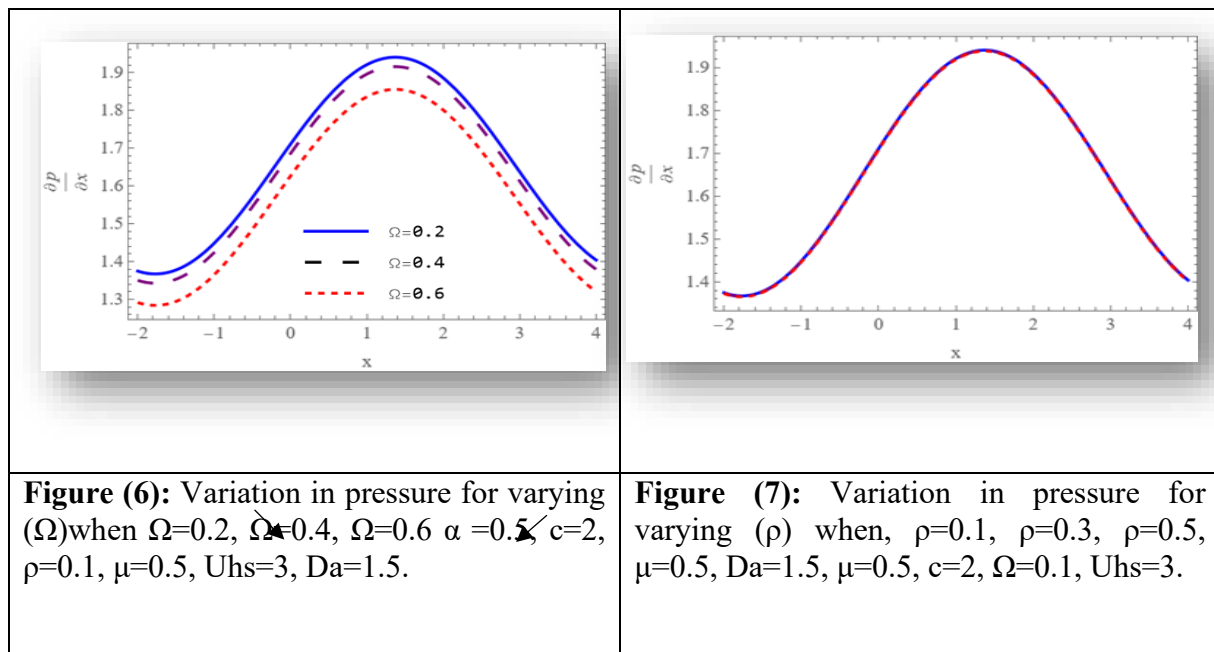
- In Figures (8), (9), and (10), the factors  $Da$  (Darcy number),  $\Omega$  (rotational parameter), and  $\rho$  (density) exhibit beneficial impacts on fluid dynamics. These parameters improve inertial contributions, raise centrifugal forces, and improve permeability. The fluid's velocity field is thus represented by the overall stream function, which tends to grow with increasing values of  $Da$ ,  $\Omega$ , and  $\rho$ . Higher stream function values are a result of increased fluid motion brought on by increased centrifugal forces and inertial contributions, as well as enhanced permeability, which permits more fluid to pass through the porous material.
- In Figures (11), (12), and (13) illustrate the effects of  $\alpha$  ( parameter of Jeffrey fluid),  $c$  (slip coefficient), and  $U_{hs}$  (electrokinetic parameter). These parameters make the stream function equal. The balance between enhancing forces (e.g., viscoelastic or electrokinetic effects) and resistive forces (e.g., slip or drag at the boundaries) determines the overall impact on the stream function. Depending on the specific system configuration, these factors can cause the stream function to increase, decrease, or remain constant. For instance, boundary slip may reduce resistance to flow, while electrokinetic forces can enhance or inhibit fluid motion depending on the charge distribution and fluid properties. Thus, the combined effects of these parameters result in non-uniform and complex behaviour in the stream function.

## 9. Velocity distribution (U)

The fluctuating value of  $u$  indicates how the axial velocity across the channel varies. The impact of various ( $Da, \Omega, U_{hs}, c, \rho, \alpha, \mu$ ) values

- In Figures (14), (15), (16), and (19), the velocity distribution increases, as a result of increases in the Helmholtz-Smoluchowski value ( $U_{hs}$ ), viscosity ( $\mu$ ), rotation rate ( $\Omega$ ), and Darcy number ( $Da$ ). The effect of  $U_{hs}$  is the most notable. Higher permeability, which lowers flow resistance and increases velocity, is indicated by an increase in  $Da$ .  $\Omega$  increases velocity by introducing centrifugal forces that create secondary flows, but its impact is smaller than that of  $U_{hs}$ . Although viscosity ( $\mu$ ) typically opposes flow, it occasionally aids in stabilizing and dispersing velocity equally, particularly when electric forces are present.
- In Figures (17) and (18), more balanced increase in velocity is seen where an increase in the slip parameter ( $c$ ) and the Jeffrey fluid parameter ( $\alpha$ ) results. A greater  $\alpha$  increases elasticity, enabling the fluid to react to applied forces faster and producing a smoother distribution of velocity. Concurrently,  $c$  lessens boundary drag, improving fluid flow and promoting a more even distribution of velocity throughout the domain





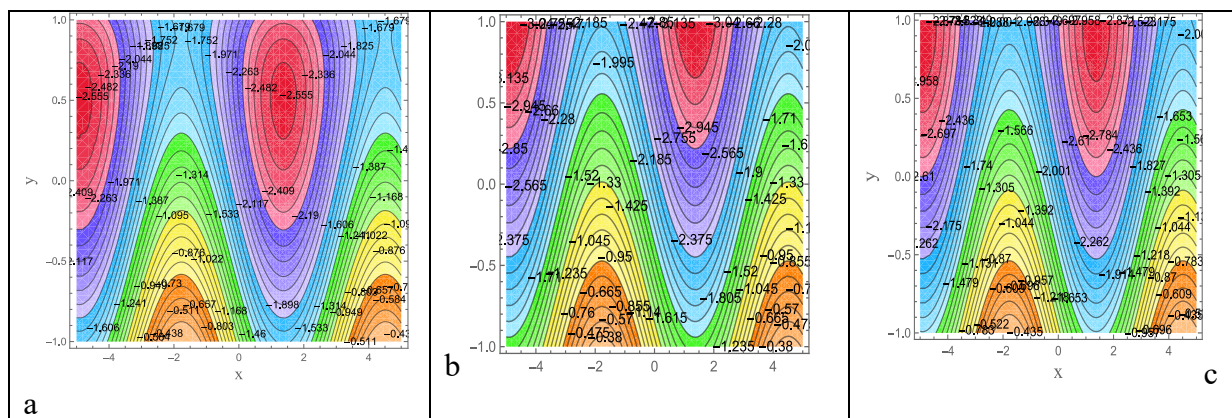


**Figure 10 :** Stream function variation for different of ( $\rho$ ) when  $\rho=0.1$   $\rho=0.3$ ,  $\rho=0.5$ ,  $\alpha=0.5$ ,  $\mu=0.5$ ,  $c=2$ ,  $\Omega=0.1$ ,  $Da=0.1$ ,  $Uhs=3$ .

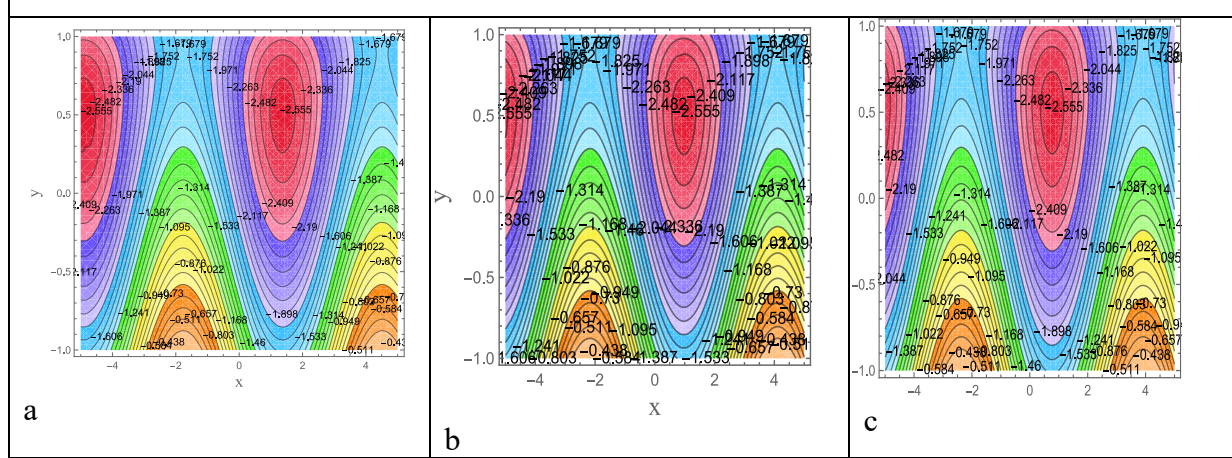


**Figure 11 :** Stream function variation for different (c), when  $c=2$ ,  $c=4$ ,  $c=6$ ,  $\rho=0.1$   $\alpha=0.5$ ,  $\mu=0.5$ ,  $\Omega=0.1$ ,  $Da=0.1$ ,  $Uhs=3$

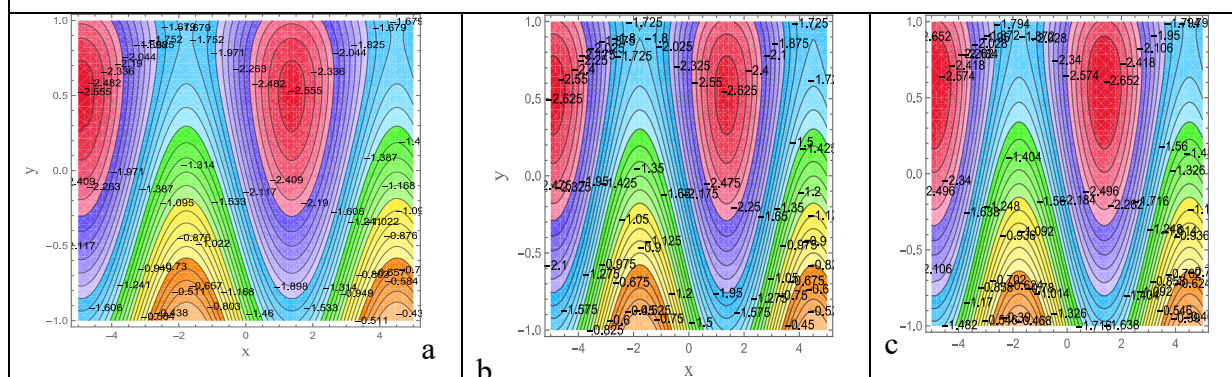


**Figure 12:** Stream function variation for different ( $\alpha$ ), when  $\alpha=0.5$ ,  $\alpha=0.7$ ,  $\alpha=0.9$ ,  $\rho=0.1$   $c=2$ ,  $\mu=0.5$ ,  $\Omega=0.1$ ,  $Da=0.1$ ,  $Uhs=3$ .

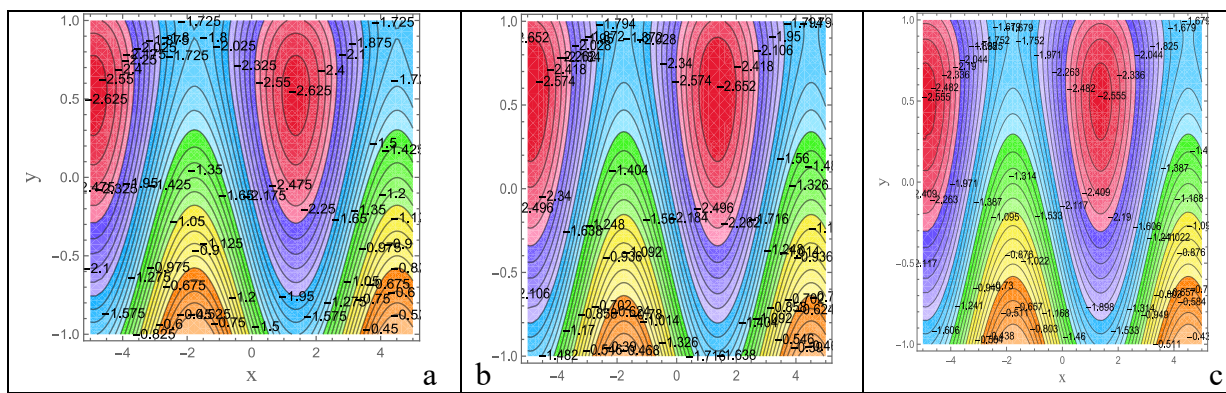


**Figure 13 :** Stream function variation for different  $U_{hs}$  when  $U_{hs}=3$ ,  $U_{hs}=4$ ,  $U_{hs}=5$ ,  $\alpha=0.5$ ,  $\rho=0.1$ ,  $c=2$ ,  $\mu=0.5$ ,  $\Omega=0.1$ ,  $Da=0.1$ .

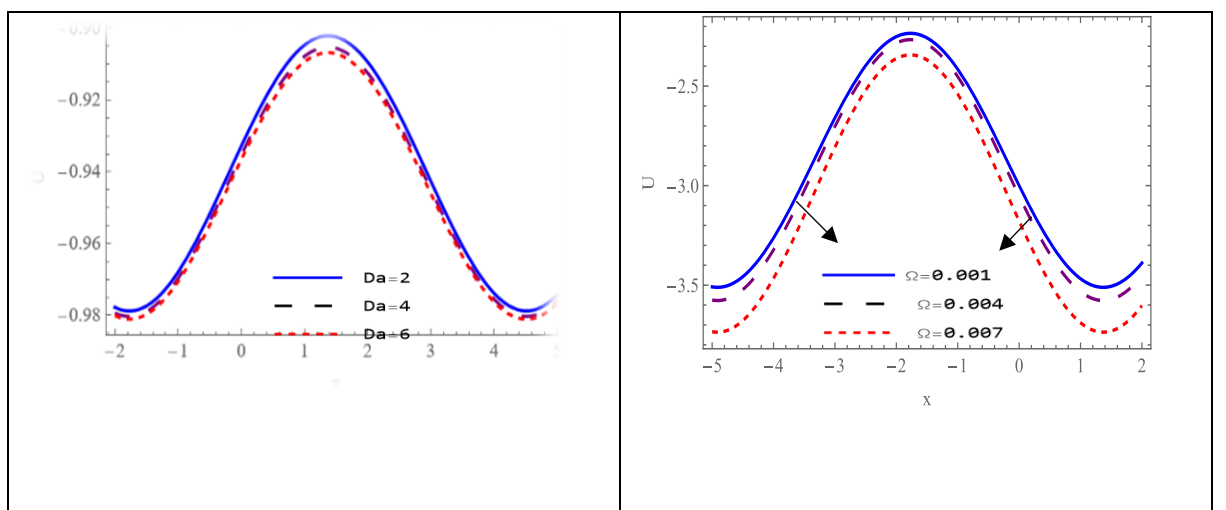


**Figure 14 :** Velocity variation for different of  $(Da)$  when  $Da=2$ ,  $Da=4$ ,  $Da=6$ ,  $U_{hs}=1.5$ ,  $\mu=0.1$ ,  $\Omega=0.1$ ,  $c=2$ ,  $\rho=0.1$ ,  $\mu=0.5$

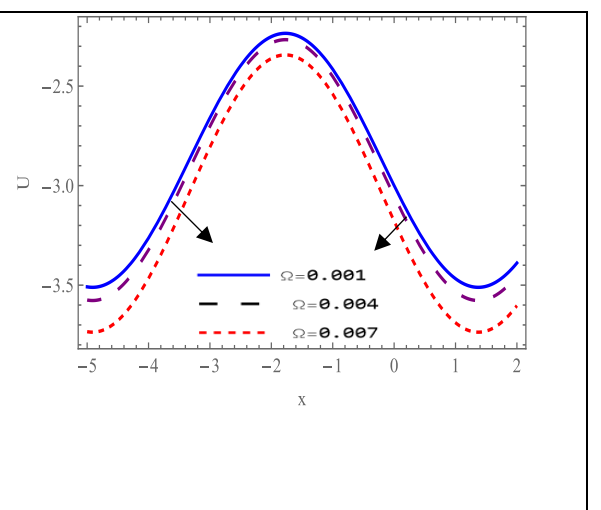


**Figure 15 :** Velocity variation for different of  $(\Omega)$  when  $\Omega=0.1$ ,  $\Omega=0.3$ ,  $\Omega=0.5$ ,  $\alpha=0.2$ ,  $Da=3$ ,  $c=0.2$ ,  $U_{hs}=3$ ,  $\mu=0.1$ ,  $c=2$ ,  $\rho=0.1$

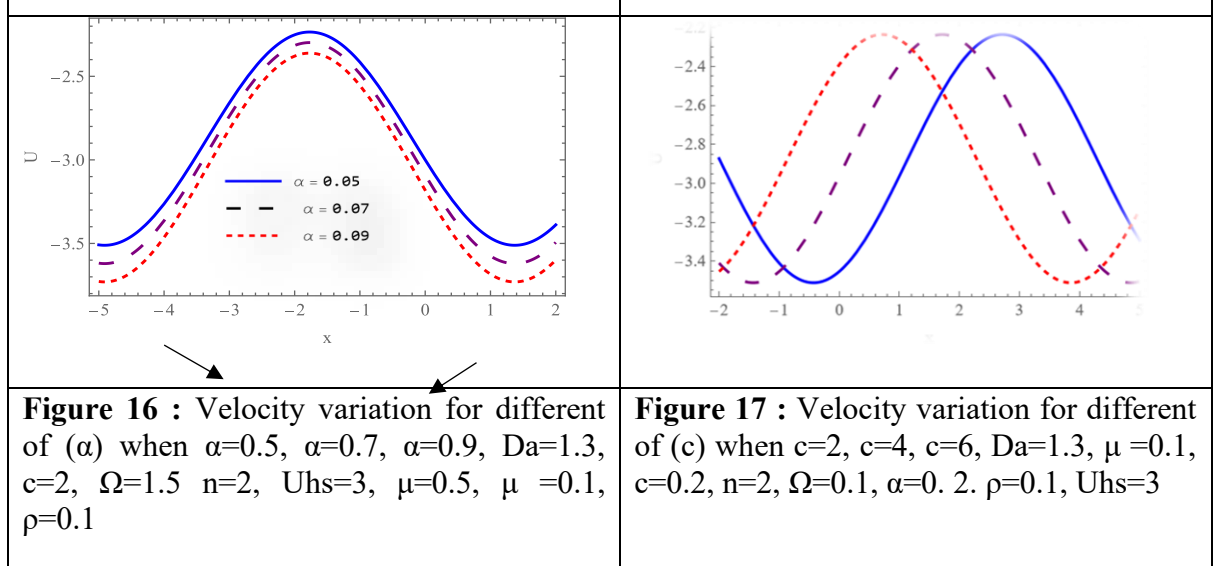


**Figure 16 :** Velocity variation for different of  $(\alpha)$  when  $\alpha=0.5$ ,  $\alpha=0.7$ ,  $\alpha=0.9$ ,  $Da=1.3$ ,  $c=2$ ,  $\Omega=1.5$ ,  $n=2$ ,  $U_{hs}=3$ ,  $\mu=0.5$ ,  $\mu=0.1$ ,  $\rho=0.1$

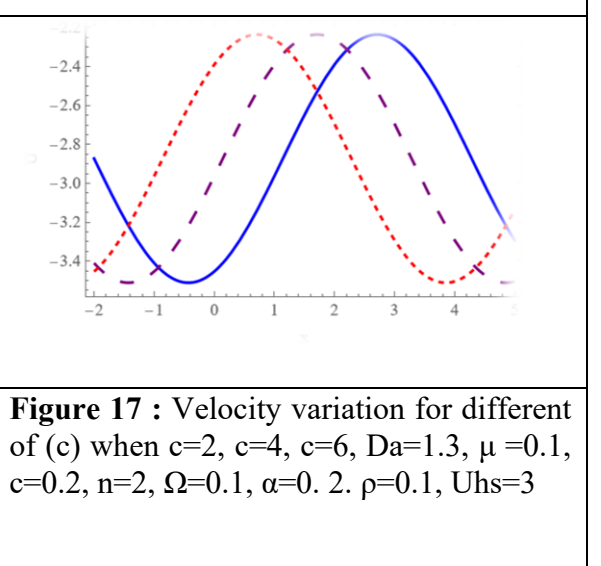
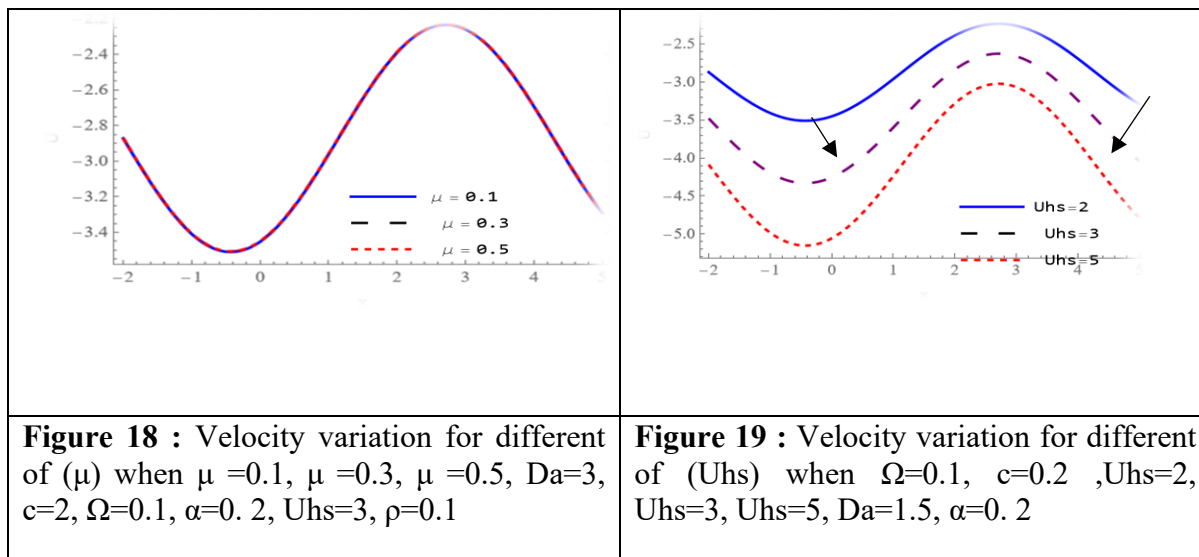


**Figure 17 :** Velocity variation for different of  $(c)$  when  $c=2$ ,  $c=4$ ,  $c=6$ ,  $Da=1.3$ ,  $\mu=0.1$ ,  $c=0.2$ ,  $n=2$ ,  $\Omega=0.1$ ,  $\alpha=0.2$ ,  $\rho=0.1$ ,  $U_{hs}=3$



## 10. Applications

Neural signaling and impulse transmission through cerebrospinal fluid are practical examples of electrical effects in action in biological systems, where the electric field is crucial for fostering neuronal connections and regulating fluid flow inside the central nervous system.



**Figure 20 :** A schematic of the transmission of neurological signals and the fluid in cerebrospinal the brain

## 11. Conclusions

This study examines how rotation affect in electric field, on the peristaltic movement of a Jeffery fluid through a porous medium within waves with different amplitudes and phases on the non-uniform walls and a low Reynolds number create the asymmetric channel. The axial velocity, pressure gradient, and stream function formulas are generated.

- A higher (Da) Darcy number value denotes greater permeability, which lowers the fluid's resistance. As a result, less pressure gradient is needed to force the fluid through the medium. The pressure gradient curve shows a decline in slope as (Da) increases in response to this.
- Stream Function and Velocity Curves: A higher (Da) results in a more uniform velocity distribution and better fluid flow. As a result of the improved fluid flow and less internal resistance, the stream function and velocity curves both rise as (Da) increases.

- As ( $\Omega$ ) rotational parameter rises, the fluid is subject to stronger centrifugal forces, which necessitate a larger pressure gradient to offset and preserve flow. This is shown as an increase in value with rising ( $\Omega$ ) in the pressure gradient curve.  $\Omega$ 's impact on Stream Function and Velocity Curves.
- A higher parameter of Jeffrey fluid ( $\alpha$ ), means that a greater pressure gradient is needed to sustain fluid flow. The pressure gradient curve has an increasing slope as  $\alpha$  increases, reflecting this phenomenon.  $\alpha$ 's effect on stream function and velocity curves. A higher viscosity causes a decrease in velocity with an increase in  $\alpha$ , which results in a less even distribution of velocity. As a result, the velocity either drops or stays constant, and the stream function curve diminishes.
- A higher (Uhs) Helmholtz-Smoluchowski value raising (Uhs) reduces the resistance and pressure gradient required for fluid flow. This is demonstrated by The pressure gradient, which decreases in value as Uhs effect on velocity curves and stream function: Because of the fluid's increased electroosmotic forces, raising (Uhs) significantly increases fluid flow which in turn enhances stream function and velocity values.
- ( $\mu$ ) The pressure gradient curve rises with increasing  $\mu$ , indicating that a bigger pressure gradient is needed to maintain fluid flow when viscosity increases. The  $\mu$ 's impact on the Velocity Curve: Higher viscosity typically results in a more even distribution of velocity across the medium and can even produce a reasonably constant velocity. This causes the velocity curve to be more balanced, with the pressure increasing.
- By emphasizing the role electric fields play in fluid dynamics and neural transmission, it highlights the interaction between neurons and fluid flow.

## References

- [1] A. M. Abd-Alla and S. M. Abo-Dahab, "Rotation effect on peristaltic transport of a Jeffrey fluid in an asymmetric channel with gravity field," *Alexandria Engineering Journal*, vol. 55, no. 2, pp. 1725-1735, 2016.
- [2] R. S. Kareem and A. M. Abdulhadi, "Impacts of Heat and Mass Transfer on Magneto Hydrodynamic Peristaltic Flow Having Temperature-dependent Properties in an Inclined Channel Through Porous Media," *Iraqi Journal of Science*, vol. 61, no. 4, pp. 11–20, 2020.
- [3] Z. A. Jaafari, L. Hummady, and M. H. Thaw, "Effects of Rotation and Inclined Magnetic Field on Walters' B Fluid in a Porous Medium using perturbation method or technique," *Iraqi Journal of Science*, vol. 63, no.2, pp. 8–10, 2024.
- [4] S. Akram and S. Nadeem, "Influence of induced magnetic field and heat transfer on the peristaltic motion of a Jeffrey fluid in an asymmetric channel: Closed form solutions," *Journal of Magnetism and Magnetic-Materials*, vol. 328, pp. 11-20, 2013.
- [5] A. W. Salih, "Influence of rotation, variable viscosity and temperature on peristaltic transport in an asymmetric channel," *Turkish Journal of Computer and Mathematics Education*, vol. 12, no. 6, pp. 11-15, 2021.
- [6] D. Gamachu and W. Ibrahim, "Entropy production on couple-stress hybrid nanofluid flow in a rocket engine nozzle with non-Fourier's and non-Fick's law," *Ain-shams Engineering Journal*, vol. 14, no. 1, pp. 12-13, 2023.
- [7] W. S. Khudair and H. H. Dwail, "Studying the magnetohydrodynamics for williamson fluid with varying temperature and concentration in an inclined channel with variable viscosity" *Baghdad Science Journal*, vol. 18, no. 3, pp. 34-37, 2021.
- [8] A. M. Jasim, "Study of the Impact of Unsteady Squeezing Magnetohydrodynamics Copper-Water with Injection-Suction on Nanofluid Flow Between Two Parallel Plates in Porous Medium," *Iraqi Jornal of Science*, vol. 63, no. 9, pp. 23-25, 2022.
- [9] H. H. Ali, "Impact of varying viscosity with hall current on peristaltic flow of viscoelastic fluid

through porous medium in irregular microchannel," *Iraqi Journal of Science*, vol. 63 no.3, pp. 1265–1276, 2022.

[10] T. W. Latham, "Fluid motions in a peristaltic pump," *Applied Mathematics*, vol. 2 no.5, pp. 11-13, 2011.

[11] T. S. Ahmed, "Effect of inclined magnetic field on peristaltic flow of Carreau fluid through porous medium in an inclined tapered asymmetric channel," *Al-Mustansiriyah Journal Science*, vol. 29, no. 3, pp. 94–105, 2018.

[12] G. G. Mhammad, "Effect of Inclined Magnetic Field on the Peristaltic Flow of Non-Newtonian Fluid with Partial Slip and Couple Stress in a Symmetric Channel," *Current Journal of Applied Science and Technology*, vol. 15 , pp. 1-11, 2016.

[13] A. Aziz, W. Jamshed, T. Aziz, H. S. Bahaidarah and K. Rehman, "Entropy analysis of Powell–Eyring hybrid nanofluid including effect of linear thermal radiation and viscous dissipation," *Journal of Thermal Analysis and Calorimetry*, vol. 143, no. 2, pp. 1331–1343, 2021.

[14] A. M. Siddiqui and W. H. Schwarz, "Peristaltic flow of a second-order fluid in tubes," *Journal of Non-Newtonian Fluid Mechanics*, vol. 53, pp. 257–284, 1994.

[15] N. A. S. Afifi and N. S. Gad, "Interaction of peristaltic flow with pulsatile fluid through a porous medium," *Applied Mathematics and Computation*, vol. 142, no. 1, pp. 167–176, 2003.

[16] E. F. Elshehawey, A. M. Sobh and M. E. Elbarbary, "Peristaltic motion of a generalized Newtonian fluid through a porous medium," *Journal of the Physical Society of Japan*, vol. 69, no. 2, pp. 401–407, 2000.

[17] A. J. Chamkha, "The Stokes problem for a dusty fluid in the presence of magnetic field, heat generation and wall suction effects," *International Journal of Numerical Methods for Heat & Fluid Flow*, vol. 10, no.1, pp. 116–133, 2000.

[18] Y. Wang, H. Chen, J. Law, X. Du and J. Yu , "Ultrafast miniature robotic swimmers with upstream motility," *Cyborg and Bionic Systems*, vol. 4, no. 15, pp. 10-21, 2023.

[19] S. R. Mahmoud, "Effect of Rotation and Magnetic Field through Porous Medium on Peristaltic Transport of a Jeffrey Fluid in Tube," *Mathematical Problemes in EngIneering*, vol. 10, pp. 1-13, 2011.

[20] G. C. Shit and S. Majee, "Computational modeling of MHD flow of blood and heat transfer enhancement in a slowly varying arterial segment," *International Journal of Heat and Fluid Flow*, vol. 70, pp. 237–246, 2018.

[21] K. Hejranfar and M. Hajihassanpour, "Chebyshev collocation spectral lattice Boltzmann method in generalized curvilinear coordinates," *Computers-and-Fluids*, vol. 146, pp. 154-173, 2017.